JOURNAL OF Materials CHEMISTRY

Influence of impurities on the properties of rare-earth-doped barium-titanate ceramics

Maya D. Glinchuk,*[a] Igor P. Bykov,[a] Sergei M. Kornienko,[a] Valentin V. Laguta,[a] Alla M. Slipenyuk,[b] Anatolii G. Bilous,†[b] Oleg I. V'yunov‡[b] and Oleg Z. Yanchevskii[b]

[a]*Department of Materials with Special Dielectric Properties, Institute for Problems of Materials Science, 03180 Kyiv, Ukraine. E-mail: glin@ipms.kiev.ua*
[b]*Department of Solid State Chemistry, V.I.Vernadskii Institute of General and Inorganic Chemistry, 03680 Kyiv-142, Ukraine*

Received 7th December 1999, Accepted 19th January 2000

Investigations of impurity centers, electrical resistivity and microstructure of $BaTiO_3$ ceramics doped with rare-earth ions Y, La, Nd, Sm, Dy and Lu at concentrations $x=0.001$–0.005 were carried out. Electron paramagnetic resonance, X-ray diffraction and electron microscopy were used for measurements. The most intense EPR lines were shown to belong to paramagnetic complexes Fe^{3+}–V_O and Ti^{3+}–Ln^{3+} (Ln = rare-earth ion, V_O = oxygen vacancy). A change in symmetry of the center Fe^{3+}–V_O at the transition temperature from the ferroelectric to paraelectric phase has been revealed for the first time. Measurements of the dependence of EPR line intensities and electrical resistivity with rare-earth ion concentrations were performed. The observed correlation in their behaviour showed an essential role of the identified paramagnetic complexes in the appearance of $BaTiO_3$ ceramic semiconducting properties and the positive temperature coefficient of resistance (PTCR) effect. The latter effect was at a maximum for $x \approx x_c$ where $x_c \approx 0.002$–0.003 is the critical rare-earth ion concentration which determines the excess charge compensation mechanism. Up to x_c, the rare earths investigated, (except for the small ion Lu), substitute for barium, and the main compensation mechanism is an electronic mechanism. At high concentrations ($x > x_c$) in the case of large ions (*e.g.* La), substitution is at barium sites, with the creation of titanium vacancies, whereas intermediate ions (*e.g.* Y) begin to substitute for titanium. The influence of impurities on the $BaTiO_3$ microstructure, including the grain sizes, is discussed.

1 Introduction

Doping of $BaTiO_3$ ceramics by rare earths or group V elements, *e.g.* niobium or tantalum, leads to the appearance of semiconductor behaviour and to a change in material properties. The most prominent of these is an anomalous increase of the electrical resistivity above the Curie temperature $T_c = 120\ ^\circ C$. This phenomenon is widely utilized in thermistors with a positive temperature coefficient of resistivity for overcurrent limiting. The possibility to govern the resistivity value by application of an external electric field (varistor effect) is important in the use of such materials. Since impurities and lattice imperfections play a crucial role in these phenomena and peculiarities of other properties, their investigation has attracted much attention.[1,2] In particular the existence of manganese, iron, chromium and other unavoidable impurities in nominally pure (undoped) $BaTiO_3$ samples was shown by EPR spectroscopy.[1,3] On the other hand, the PTCR effect exhibited by donor-doped $BaTiO_3$ ceramics (*e.g.* with rare-earth ions or Nb, Ta ions) can be enhanced by the addition of a small amount of 3d elements, the most effective being Cu or Mn, leading to a higher resistivity ratio ρ_{max}/ρ_{min}.[2,4] 3d-Metal ions substituted for Ti^{4+} are usually acceptors and hence act as traps for carriers. It is important to consider the influence of donor and acceptor impurities on one another and on the ceramic properties of $BaTiO_3$. The mutual influence of impurities and lattice defects follows from the necessity of excess charge compensation. The latter can result in a change of impurity ion charge and position in the lattice and appearance of Ti^{3+}, as observed previously in doped lead zirconate–titanate (PZT) ceramics.[5,6] All these phenomena in the impurity subsystem can strongly influence properties of the material. It is known that doping of $BaTiO_3$ by 1 atom% La^{3+} leads to the appearance of titanium vacancies with Ba ion substitution, whereas Y^{3+} ions can substitute both in barium and titanium sublattices.[7,8] However these models do not explain the onset of semiconducting properties in $BaTiO_3$ with small dopant concentrations.

In the present work, investigations of impurity centers, the dependence of electrical resistivity on temperature, concentration of rare-earth ions and dc electric field and concentration dependence of grain size were carried out for $BaTiO_3$ ceramics doped with rare-earth ions.

Electron paramagnetic resonance (EPR), X-ray diffraction (XRD) and electron microscopy were used for measurements. The observed dependence of EPR spectra intensity and paramagnetic center types on rare-earth ion concentration and temperature and correlation between EPR line intensity and electrical resistivity allowed analysis of the influence of impurities on the properties of $BaTiO_3$ ceramics.

2 Samples and experimental details

Ceramic samples of $BaTiO_3$ doped with Y, La, Nd, Sm, Dy and Lu were fabricated by a conventional solid-phase reaction technique. Extra pure $BaCO_3$ (purity $>99.999\%$),§ TiO_2 (purity $>99.99\%$),¶ Y_2O_3, La_2O_3, Nd_2O_3, Sm_2O_3, Dy_2O_3

†E-mail: belous@mail.kar.net
‡E-mail: vyunov@ionc.kar.net

§Donetsk plant for chemical reagents, Donetsk, Ukraine; Manufacturer's analysis: Fe <3 ppm, Mn <3 ppm, Cu <1 ppm.
¶"Krasnyi Khimik", St. Petersburg, Russia; Manufacturer's analysis: Fe <3 ppm, Al <2 ppm, Ca <4 ppm.

DOI: 10.1039/a909647g

and Lu_2O_3 (purity $>99.99\%$) were used. The temperature of synthesis was chosen such that the concentration of free barium oxide after the first treatment was $\leqslant 1\%$. The rare-earth ion content in the samples was 0.001, 0.002, 0.003, 0.004 or 0.005 for any impurity; these values correspond to concentrations of 0.1, 0.2, 0.3, 0.4 and 0.5 atom%. The ratio of components was taken in accordance with the formula $Ba_{1-x}Ln_xTiO_3$. In order to ensure liquid-phase sintering, a sufficient amount of TiO_2 was added to produce 1 atom% excess of Ti over the stoichiometric quantity.[9] A small amount of SiO_2 was also added as a sintering aid.[10] The pellet specimens of *ca.* 3 mm thickness and 10 mm diameter were prepared by a semidry molding method with an organic binder and sintered at 1340–1360 °C in air atmosphere. The cooling rate for all samples was 300 °C h^{-1}. The ohmic contacts for resistivity measurements were fabricated by firing Al paste. The phase content of the materials obtained was examined by XRD of the powders and grain sizes were measured using a JCXA Superprobe 733 microanalyzer. EPR spectra were recorded between 160 and 480 K on a spectrometer operating at $\nu = 9.4$ GHz. Powder samples were used during EPR spectra measurements. Effective *g*-factor values were calculated with the use of the equation, $h\nu = g\beta B_r$, where B_r is the resonance magnetic field, determining the line position.

3 Results of measurements

3.1 EPR spectra

EPR spectra observed at $T = 300$ K in $BaTiO_3$ ceramics, both nominally pure and slightly doped with rare-earth ions are shown in Fig. 1. Characteristic spectra of Mn^{2+} and Fe^{3+} were observed[11–14] but the most intense lines were shown to belong to other centers, which had *g*-factors of *ca.* 5.549 and 1.963 in undoped $BaTiO_3$. These are now considered in more detail.

3.1.1 EPR signal with $g \approx 5.549$. It is most probable that this line belongs to a tetragonal symmetry paramagnetic center Fe^{3+}–V_O. Such a spectrum could be the result of spin level splitting by the large tetragonal crystalline field produced by an oxygen vacancy V_O, so that only one line at $g \approx 5.549$ ($B \approx 100$ mT) can be observed. This line is usually described by the effective spin-Hamiltonian $H_{eff} = g_{eff}\beta B S_{eff}$ with effective spin $S_{eff} = 1/2$. This type of spectrum is observed for all centers with oxygen vacancies, and has been studied in much detail for Fe^{3+}–V_O and Mn^{2+}–V_O in $SrTiO_3$.[15] The EPR spectrum of Fe^{3+}–V_O in $BaTiO_3$ single crystals has been observed previously in samples doped with iron at $T = 20$ K (rhombohedral phase).[3] In the tetragonal phase this signal was observed in $BaTiO_3$ ceramic samples doped with niobium and iron, whereas there was no such spectrum in samples additionally doped by Sn.[16,17]

We have observed, for the first time, an EPR spectrum of Fe^{3+}–V_O (Fig. 1) in $BaTiO_3$ ceramic samples, which were nominally pure or doped by rare-earth ions only. The temperature dependence of the parameters of this spectrum was investigated. The EPR signal of the Fe^{3+}–V_O center appeared in the tetragonal phase while above $T \approx 350$ K it began to broaden with increasing temperature (Fig. 2). The temperature dependence of the line width ΔB was shown to obey the Arrhenius law:

$$\Delta B(T) = \Delta B \exp(-E_a/kT) \quad (1)$$

with activation energy $E_a = 0.5$ eV and $\Delta B = 2.54 \times 10^{13}$ Hz obtained from the dependence of $\ln[\Delta B(T)]$ with reciprocal temperature ($1/T$) as shown in the insert to Fig. 2.

The most interesting and unexpected phenomenon was the disappearance of the Fe^{3+}–V_O EPR signal at the transition temperature T_c to the cubic phase. It should be noted that in $SrTiO_3$[15] this spectrum was observed both in cubic and in tetragonal symmetry phases. In $BaTiO_3$ samples the Fe^{3+}–V_O EPR spectrum disappeared at T_c, and simultaneously a cubic symmetry Fe^{3+} center EPR signal was observed at $T > T_c$. To the best of our knowledge this is the first observation of such behaviour for an impurity complex containing vacancies at the transition temperature from the para- to the ferro-electric phase.

We revealed also an interesting dependence of Fe^{3+}–V_O EPR signal intensity and *g*-factor on rare-earth ion type and concentration (Table 1) as shown in Fig. 3(a). It is seen that the intensity of Fe^{3+}–V_O EPR signal decreases with concentration up to a value close to $x_c = 0.002$ and remains practically constant at $x > x_c$. This behaviour is characteristic of all rare-earth ions except Lu [see Fig. 3(a)]. In section 4 we discuss possible reasons of the observed phenomena.

3.1.2 EPR signal with $g \approx 1.963$. This signal intensity increases with rare-earth ion concentration [Fig. 3(b)], whereas in pure $BaTiO_3$ it is very weak. The *g*-factor of the signal is close to that of Ti^{3+} but shows some differences from all previously characterized examples.[18] As a consequence, the EPR signal near $g \approx 1.963$ was assigned to the complex center Ti^{3+}–Ln^{3+}, where Ln is a rare-earth ion substituted for Ba^{2+}. Clearly this center arises from charge compensation. In undoped (pure) $BaTiO_3$ small amounts of unavoidable impurities with excess positive charge in the lattice may also lead to a weak Ti^{3+}–M^{n+} signal. The reason of the appearance

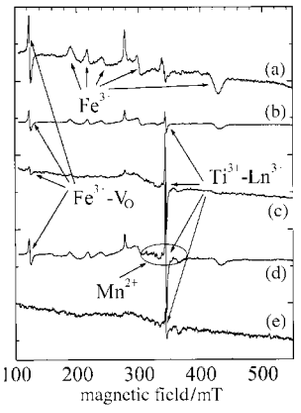

Fig. 1 EPR spectra of pure $BaTiO_3$ ceramic (a) and $BaTiO_3$ ceramics doped by 0.001 Lu (b), 0.001 La (c), 0.001 Dy (d), 0.002 Sm (e); $T = 20$ °C.

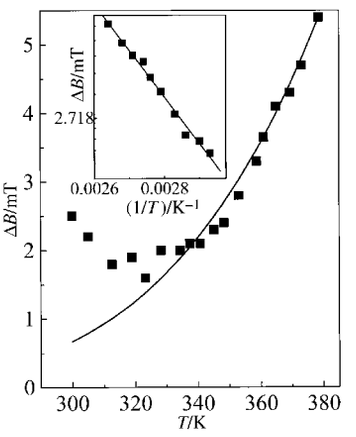

Fig. 2 EPR line width of the Fe^{3+}–V_O center in undoped $BaTiO_3$ ceramic *vs.* temperature; (■) experimental points, (—) calculation on the basis of eqn. (1).

Table 1 *g*-Factors of Fe^{3+}–V_O centers in $BaTiO_3$ with different dopants at $T=300$ K (for pure $BaTiO_3$, $g=5.549$)

	x				
Ln	0.001	0.002	0.003	0.004	0.005
Y	5.578	5.573	5.568	—[a]	—[a]
Lu	5.588	5.533	5.542	—[b]	5.518
Dy	5.584	—[a]	—[a]	5.512	5.525
Sm	5.551	—[a]	—[b]	5.493	5.479
Nd	5.55	—[a]	—[a]	5.424	5.437
La	5.532	—[b]	5.481	5.516	5.423

[a]No spectrum observed. [b]Sample not prepared.

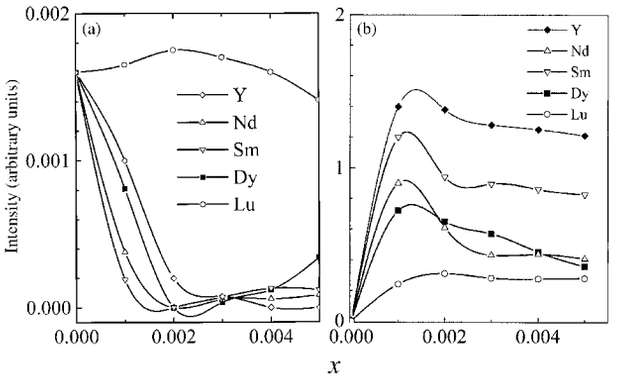

Fig. 3 EPR line intensity of Fe^{3+}–V_O (a) and Ti^{3+}–Ln^{3+} (b) centers in $BaTiO_3$ ceramics *vs.* the rare-earth element content, *x*; $T=20$ °C.

of Ti^{3+}–Ln^{3+} centers would be the necessity of charge compensation for the rare-earth ion. The dependence of this EPR signal intensity on rare-earth ion concentration is depicted in Fig. 3(b). After a sharp increase at $x<0.001$ the intensity decreases slowly at $x\leqslant x_c$. The value of the *g*-factor of this center changes slightly with *x* up to $x=x_c=0.002$ while at $x>x_c$ its value remains practically constant (Table 2). The temperature dependence of the EPR spectra shows the existence of this center both in the tetragonal and cubic phase. Reduction in intensity of this center would be caused by low spin–lattice relaxation times, known to be characteristic of Ti^{3+} at high enough temperatures.

3.2 Physical–chemical properties of doped $BaTiO_3$ materials

Measurements of the influence of rare-earth ion concentration on electrical resistivity, the grain size, effective lattice constant and dc electric field influence on resistivity were carried out at room temperature. The influence of temperature on the value of electrical resistivity between 0 and 400 °C was studied for the rare-earth ions of Y, La, Nd, Sm, Dy and Lu at several concentrations. Since the behaviour of the resistivity for all of them except Lu was qualitatively similar, we present here the results only for La_2O_3 and Nd_2O_3 doped $BaTiO_3$ ceramics.

Table 2 *g*-Factors of Ti^{3+}–Ln^{3+} centers in $BaTiO_3$ with different dopants at $T=300$ K

	x				
Ln	0.001	0.002	0.003	0.004	0.005
Y	1.962	1.97	1.972	1.971	1.972
Lu	1.969	1.97	1.971	—[a]	1.971
Dy	1.964	1.972	1.973	1.965	1.971
Sm	1.965	1.971	—[a]	1.971	1.971
Nd	1.97	1.971	1.971	1.971	1.975
La	1.963	—[a]	1.972	1.965	1.971

[a]Sample not prepared.

3.2.1 Electrical resistivity. Doping of $BaTiO_3$ ceramics by rare-earth ions leads to the appearance of semiconducting properties and electrical resistivity changes. Fig. 4 shows that at room temperature the resistivity decreases by several orders of magnitude with increasing concentration of *x* up to $x\leqslant0.002$. Minimum resistivity is observed at a concentration of *ca.* 0.002, with increase in resistivity then being observed with concentration of rare-earth ions except for Y, for which an increase in resistivity is observed at higher concentrations (see Fig. 4).

The most significant property of the $BaTiO_3$ ceramics is the strong increase in resistivity at $T\geqslant T_c$ with a positive temperature coefficient as depicted in Fig. 5 for $BaTiO_3$ samples doped with La_2O_3 (a) and Nd_2O_3 (b). The jump of resistivity however disappears for $x=0.003$ (Fig. 4). Samples with $x\approx0.002$, which have the smallest resistivity at room temperature, are most suitable for application in devices for overcurrent limiting whereas samples with larger resistivity at room temperature may be useful for the production of heaters.

3.2.2 Varistor effect. Investigations of the influence of a dc external electric field on sample resistivity shows a decrease in resistivity with increase in field. The magnitude of this varistor effect depends on temperature: it is larger in the paraelectric phase than in ferroelectric phase because of a strong internal

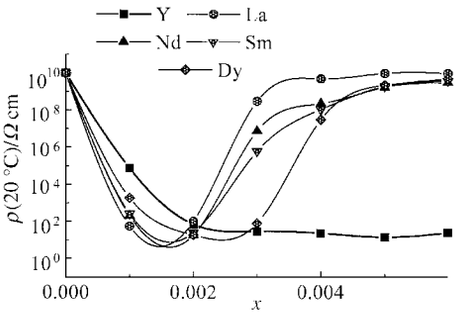

Fig. 4 Resistivity of $BaTiO_3$ ceramics doped with rare-earth ions *vs.* the degree of aliovalent substitution, *x*; Ln = Y (a); La (b); Nd (c); Sm (d); Dy (e); $T=20$ °C.

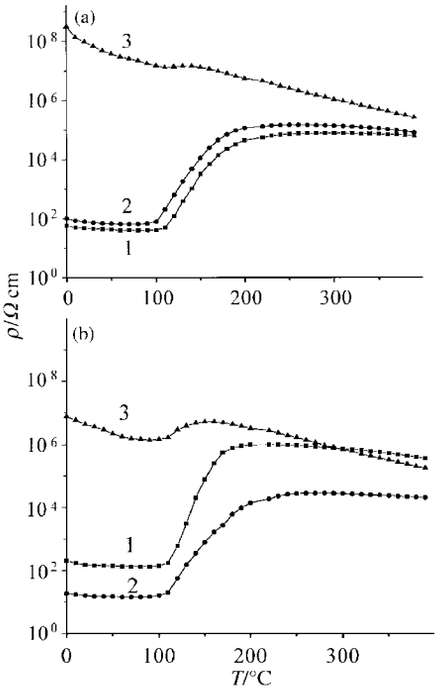

Fig. 5 Resistivity of barium titanate doped with La_2O_3 (a) and Nd_2O_3 (b) *vs.* temperature; $x=0.001$ (1); 0.002 (2); 0.003 (3).

electric field, arising in the ferroelectric phase, which is associated with spontaneous polarization. Study of the varistor effect in the paraelectric phase ($T=300\,^{\circ}C$) revealed its dependence on the identity and concentration of rare-earth ions (*cf.* Fig. 6(a) and (b)). The resistivity is seen to decrease with increasing concentration of La and Nd.

3.2.3 Microstructure. XRD investigations of $BaTiO_3$ samples doped with rare-earth ions were carried out. Fig. 7 shows a section of the diffractograms of samples doped with Nd ions. The decrease in splitting of peaks 422 and 224 at $x>0.03$ along with asymmetrical peak broadening may be the consequence of coexistence of cubic and tetragonal phases in the ceramics. These results are similar to those previously obtained for La-based ceramics.[19] Curves 1–3 in Fig. 7 relate to tetragonal single-phase samples, whereas curves 4 and 5 indicate two-phase samples. Note that similar results were obtained previously when substituting La for Ba.[20]

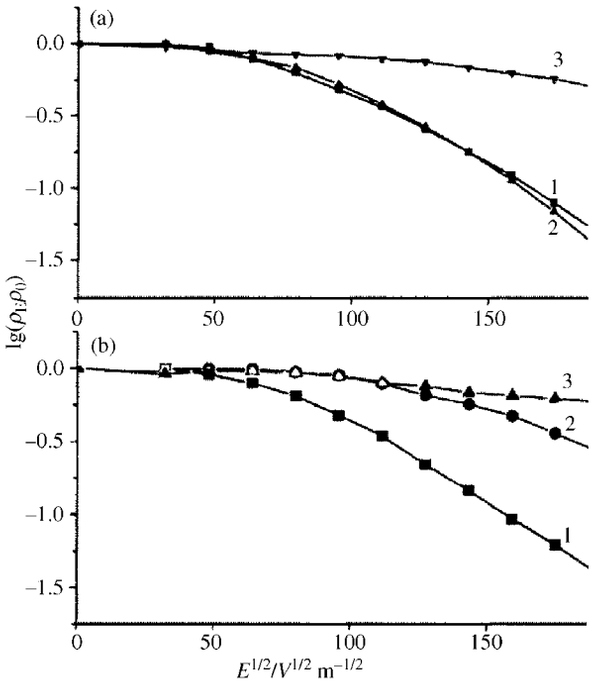

Fig. 6 Logarithm of the normalized resistivity of barium titanate doped with La_2O_3 (a) and Nd_2O_3 (b) *vs.* electric field strength, E; $x=0.001$ (1); 0.002 (2); 0.003 (3). $T=300\,^{\circ}C$.

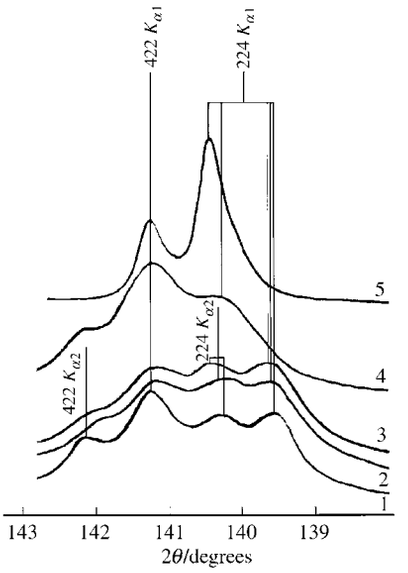

Fig. 7 Region of the XRD pattern for $BaTiO_3$ ceramics doped with Nd ions; $x=0.001$ (1); 0.003 (2); 0.005 (3); 0.03 (4); 0.04 (5). $T=20\,^{\circ}C$.

An unusual concentration dependence of the adjusted lattice parameter $\bar{a}=(a^2c)^{1/3}$ was observed in doped $BaTiO_3$ in the range of x where samples are monophasic and tetragonal. Fig. 8 shows this dependence for Nd and La doped samples. The existence of a maximum is clearly seen at $x\approx0.002$. Previously, the maximum of $\bar{a}$ was observed in Gd doped samples at $x\approx0.001$, connected with the maximum of lattice parameter c at this concentration.[21] As yet, the physical reasons of this behaviour are not known.

Since for ceramic material properties the grain size and hence intergrain space are known to play an important role, we performed measurements of the influence of rare-earth ion concentration on the grain size. Fig. 9 shows micrographs obtained for $BaTiO_3$ doped with Nd. A decrease in grain size with an increase in Nd concentration is clearly observed.

4 Discussion

4.1 Peculiarities of the behaviour of Fe^{3+}–V_O impurity centers

The observed temperature dependence of Fe^{3+}–V_O EPR line width seems to be unusual. As was stated in section 3.1.1, the broadening of the line obeyed the Arrhenius law [eqn. (1)] with parameters expected for jumping over the barrier of a lattice defect or an impurity. In the complex Fe^{3+}–V_O this would correspond to the motion of oxygen vacancy between six equivalent positions near Fe^{3+} substituted for Ti^{4+}. The vacancy must be tied to Fe^{3+} ions at least up to $T\approx400$ K, *i.e.* up to the transition temperature T_c owing to the persistence of the tetragonal symmetry of the center.

What was more unexpected was a sudden change in spectral symmetry from tetragonal to cubic at $T>T_c$. The reason of this behaviour may be a change in the oxygen vacancy energy level at $T>T_c$. Theoretical calculations had shown that in $PbTiO_3$ the energy level of V_O along the spontaneous polarization direction is 0.3 eV lower than for a vacancy in the direction normal to polarization.[21] Since the dipole moment of the pair defect Fe^{3+}–V_O must be oriented along the spontaneous polarization in $BaTiO_3$ ceramics, one can suppose that the aforementioned reasons are also correct for $BaTiO_3$ *i.e.* these pair defects have to be stable enough in the ferroelectric phase.

High enough permittivity and the disappearance of spontaneous polarization at $T\geqslant T_c$ may result in lower energy of the vacancies in the ferroelectric phase than in the paraelectric phase. Therefore the transformation of axial symmetry Fe^{3+}–V_O centers into cubic symmetry Fe^{3+} centers at $T>T_c$ may be connected with the removal of oxygen vacancies.

Another possibility for the transformation of axial spectra into cubic spectra could be averaging of axiality due to fast reorientation of vacancies near the Fe^{3+} ions. This phenomenon is usually manifested by EPR line narrowing, whereas we observed broadening of the line (see Fig. 2). Estimation of criteria of motional narrowing $\Delta\omega\tau<1$ [$\Delta\omega=(B_{\parallel}-B_{\perp})g\beta/h$ and $1/\tau$ are the separation of the components tetragonal spectra and vacancy reorientation rate, respectively] shows that for reorientation rate given by eqn. (1) averaging of the axial spectra to cubic symmetry would be expected only at $T>500$ K. However, polarization increases the barrier height so that it will be lower in the paraelectric phase. This would lead to an increase in vacancy reorientation rate and hence to the fulfillment of motional narrowing criteria at lower temperatures close to $T=T_c$.

Therefore, we have observed for the first time a new critical phenomenon: the transformation of Fe^{3+}–V_O axial centers during the ferro-para-electric phase transition. The absence of this phenomenon for the $SrTiO_3$ incipient ferroelectric ceramic

confirms the essential role of polarization in this phenomenon. Addition of rare-earth ions changes not only the Fe^{3+}–V_O EPR signal intensity, but also its position, *i.e.* the effective *g*-factor (see Table 1). The latter may be a consequence of crystalline field changes induced by rare-earth ions.

4.2 Positions of rare-earth ions in the lattice

The observed concentration dependence of the Fe^{3+}–V_O EPR signal intensity at $T=300$ K [Fig. 3(a)] indicates that at low concentrations of rare-earth ions, namely at $x<x_c\approx0.002$, which corresponds to the minimum in the curves, all rare earth ions except Lu substitute for Ba^{2+}. To compensate the excess positive charge, the number of Fe^{3+}–V_O centers, which also leads to excess positive charge to the lattice, must be decreased. It is most probable that the process Fe^{3+}–$V_O\rightarrow Fe^{2+}$–V_O takes place since an increase of cubic Fe^{3+} EPR spectrum intensity was not observed. Therefore we propose that electrons are trapped by Fe^{3+} ions and such transformation of Fe^{3+} ions to Fe^{2+} ions has been observed previously.[18] Note that at 9.4 GHz it is impossible to observe Fe^{2+} by EPR spectroscopy. At $x=x_c\approx0.002$ the Fe^{3+}–V_O centers have disappeared, with complete reduction to Fe^{2+} likely to have occurred. Similar behaviour has been observed previously in $PbZr_{1-x}Ti_xO_3$ ceramics doped with La which substituted for A or B ions at $y<0.04$ or $y>0.04$, respectively (y is the La ion content).[22]

It follows from Fig. 3(a) that the variation of Fe^{3+}–V_O intensity in samples doped with Lu^{3+} differs from the other Ln^{3+} dopants, and the line intensity only slightly depends on Lu^{3+} concentration. This can be explained by the assumption that Lu^{3+} substitutes for both A and B ions at all the concentrations studied, so that no excess charge is generated. This different behavior may be a consequence of the smaller ionic radius of Lu^{3+} relative to the other Ln^{3+} ions. The possibility of other rare-earth ions substituting for both Ba and Ti ions in the $BaTiO_3$ lattice should depend on the ratio of their ionic radii. Because of the small ionic radius of Ti ions a compensation mechanism involving the appearance of Ti vacancies ($V_{Ti}^{''''}$) and Ln^{3+} in Ba^{2+} sites cannot be ruled out. $V_{Ti}^{''''}$ sites would induce a negative excess charge (-4), which could compensate four Ln^{3+}(Ba^{2+}) ions at a distance of 1–3 lattice constants from the vacancy. Such clusters may result in a reasonably substantial change of the properties of the material and may account for a change in doped Lu ceramic grain size, which was also observed in ref. 23. Keeping in mind that random elastic fields induced by ionic radii differences have a shorter range of action than electric fields induced by excess charges, the latter seems to be more important in affecting lattice stability. EPR spectra have never been observed for $V_{Ti}^{''''}$ centers even in strongly doped $BaTiO_3$.[18] One can suppose, however, that such centers would occupy intergrain spaces where their excess charge can be compensated by various impurities and imperfections. Strong disorder in intergrain spaces results in very broad and low intensity EPR lines, so that they would be difficult to observe. The fairly intense spectra observed in our samples are most probably from paramagnetic centers in intragrain regions.

4.3 Dipole complex Ti^{3+}–Ln^{3+}

An EPR signal with $g=1.963$ in $BaTiO_3$ ceramics slightly doped by La ($x<0.001$) has been observed previously[24] the origin of which was supposed to be from electrons localized near oxygen vacancies. This may correspond to F-center like species with the carrier smeared between two nearest Ti^{4+} ions or a Ti^{3+}–V_O center if the electron is trapped by one of two Ti^{4+} nearest the vacancy. For F-centers the *g*-factor is known to be 2.0023, which strongly differs from the observed value. On the other hand, no Ti^{3+} centers investigated in undoped $BaTiO_3$ samples have $g\approx1.963$.[18] Therefore the model of the paramagnetic center proposed in ref. 24 is not reasonable. In our opinion, our assignment of Ti^{3+}-Ln^{3+} is more probable. As can be seen from Figs. 1 and 3(b), this signal has a very low intensity in pure $BaTiO_3$. Its intensity increases with rare-earth ion concentration up to $x=x_c$ and is practically constant at $x>x_c$. This behaviour is in good agreement with the conclusions stated above relating to the change of compensation mechanism at $x\approx x_c$. According to literature data, the mechanism of substitution of rare-earth ions for cations in barium titanate is dependent on rare-earth ion size.[23] For ions with large ionic radius (*e.g.* La), substitution below the critical concentration x_c takes place in the barium sublattice with electronic compensation. Above x_c, the rare-earth ions remain in the barium sublattice, and compensation involves the formation of $V_{Ti}^{''''}$ centers.[25]

For rare-earth ions with medium ionic radius (*e.g.* Y, Dy), substitution below the critical concentration x_c takes place in the barium sublattice with electronic compensation. Above x_c, the rare-earth ions substitute for titanium, substitution at the Ti site becoming increasingly preferential when moving along the rare-earth series towards smaller ions.[8] Ions with small ionic radius (*e.g.* Lu) substitute simultaneously for barium and titanium.[26] The consequence of this is clearly seen in Fig. 3(a). It should be underlined that the centers Ti^{3+}(B)–Ln^{3+}(A) as well as Ln^{3+}(A)–Ln^{3+}(B) (where M^{3+}(A or B) is an ion in A or B site) are electric dipoles in the lattice. The magnitude of the dipole moments is $e\times d$, where e is the charge of an electron d is the distance between the A and B sites. It is most probable that for dipole complexes Ti^{3+}–Ln^{3+} that $d=a\sqrt{3/2}$ where a is the lattice constant, whereas d values for other dipole complexes can be larger. Destruction of Ti^{3+}–Ln^{3+} centers as a consequence of the ferroelectric-paraelectric phase transition would lead to the disappearance of the EPR signal on the basis of the same reasons discussed earlier for the Fe^{3+}–V_O centers. A high spin–lattice relaxation rate as mentioned in section 3 may also contribute to reduction of EPR intensity for this signal.

4.4 Anomalies of physical properties

4.4.1 Influence of impurities on microstructure. EPR data have shown that the excess positive charge induced by substitution of Ln^{3+} ions for Ba^{2+} at $x<x_c\approx0.002$ is compensated for by formation of Ti^{3+} (as well as unavoidable impurity ions such as Fe^{3+}, Fe^{2+}, Mn^{2+}). At $x>x_c$ some Ln^{3+} ions (*e.g.* Y) retain their positions in A sites, and other Ln^{3+} ions substitute for Ti^{4+} ions. As a result, complexes Ln^{3+}(A)–Ln^{3+}(B) with electric dipole moments can arise. The decrease in grain size with x, clearly seen in Fig. 9 at $x\geqslant0.002$, may be due to the appearance of such complexes as well as La^{3+} (Ba^{2+})–$V_{Ti}^{''''}$. Such species probably occupy mainly intergrain spaces, whereas Fe^{3+}–V_o centers would be in intergranular regions. The absence of Fe^{3+}–V_O centers at $x>x_c$ is because of reduction of Fe^{3+} to Fe^{2+} and the resulting Fe^{2+}–V_O centers are mainly in enlarged intergrain regions.

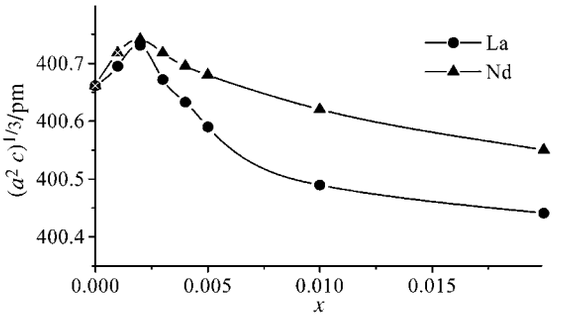

Fig. 8 Reduced lattice parameters for $BaTiO_3$ ceramics doped with rare-earth ions *vs.* the degree of aliovalent substitution x.

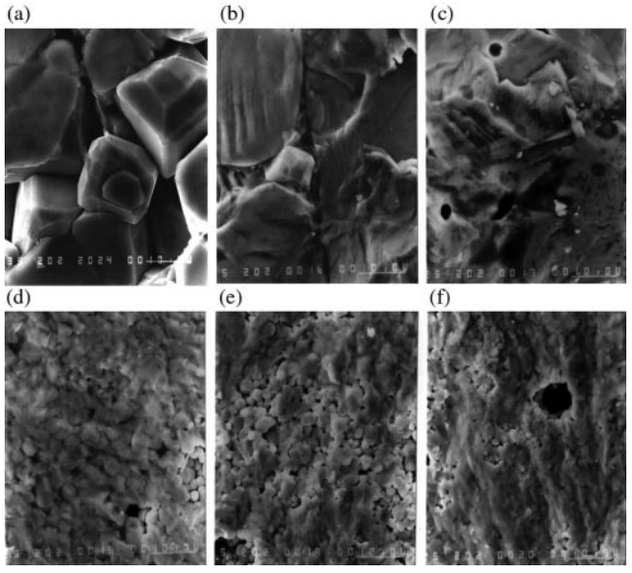

Fig. 9 Microstructure of $BaTiO_3$ ceramics doped by Nd ions *vs.* the degree of aliovalent substitution: $x=0$ (a); 0.001 (b); 0.002 (c); 0.003 (d); 0.004 (e); 0.005 (f).

Therefore there is a relation between impurity concentration, charges, positions and grain size in doped $BaTiO_3$ ceramics, similar to what we observed previously in PZT ceramics doped with Nb and Mn.[5] On the other hand, the distribution of the grain sizes (see Fig. 9) may lead to the coexistence of tetragonal and cubic phases as was suggested previously.[27] Random electric fields induced by electric dipole complexes and impurities may be a source of XRD peak broadening as well leading to the transformation of the ferroelectric tetragonal phase into the paraelectric cubic phase.[28] Such random electric fields may also influence the grain size. The maximum of the value of the adjusted parameter $\bar{a}=(a^2c)^{1/3}$ (Fig. 8) may be due to the appearance of Ti^{3+} ions since their ionic radius is larger than that of Ti^{4+}. As can be seen from Figs. 3(b) and 8 the position of the EPR signal maximum for Ti^{3+}-Ln^{3+} is similar to that of the adjusted parameter maximum. Complexes Ti^{3+}–Ln^{3+}, revealed in this work for the first time, suggest that the doping of $BaTiO_3$ by rare-earth ions leads to the formation of rare-earth titanates with the formula $Ln^{3+}Ti^{3+}O_3$.

Note that in accordance with X-ray fluorescence data, the concentration of unavoidable impurities such as iron or manganese was *ca.* 100 ppm in our samples, which is much lower than the rare-earth ion content in doped samples. Thus, the origin of the conductivity and semiconducting properties of $BaTiO_3$ ceramics sintered in air atmosphere is from rare-earth ions and lattice defects such as Ti^{3+} rather than unavoidable impurities such as Fe^{3+}. The presence of the Ti^{3+}–Ln^{3+} EPR spectrum intensity maxima near the rare-earth ion concentration, which corresponds to the resistivity minima [see Figs. 3(b) and 4], is also in accord with this. On the other hand, even low concentration of unavoidable impurities (*e.g.* iron, manganese) can play an important role in PTCR effects.

4.4.2 PTCR effect. The most prominent anomaly of doped $BaTiO_3$ ceramics is the PTCR effect and many authors have discussed the mechanism of this effect. Among them, Heywang's model is the most widely cited, in which the increase in resistivity is attributed to increase in potential barriers at grain boundaries induced by impurities.[29] On the other hand, a resistivity jump near $T\cong T_c$ gives evidence about the influence of polarization on this phenomenon as was proposed by Jonker.[30] It was shown recently that Heywang's model is adequate for the explanation of resistivity behaviour at $T>T_c$, when the resistivity slowly increases whereas at $T\cong T_c$ the main role is played by acceptor centers such as Mn–V_O.[2] The observed changes of EPR spectral intensity at $T\cong T_c$ confirm this statement.[2–4] In these studies in which $BaTiO_3$ ceramics were doped by Mn ions the change in the energy level of centers such as Mn–V_O near $T\cong T_c$ was proposed as the main reason of the resistivity jump with concentration of dopant.

In the present work, we investigated $BaTiO_3$ ceramics doped with rare-earth ions only. In such samples we observed a correlation between Fe^{3+}–V_O center intensity and resistivity value [see Figs. 3(a) and 4]. This fact, and the absence of Fe^{3+}–V_O centers and a PTCR effect at $x>x_c$ [see Figs. 3(a) and 5] suggest the involvement of Fe^{3+}–V_O centers in the resistivity jumps. At $T<T_c$ the electric dipole moments of these centers are oriented along the spontaneous polarization direction which stabilizes the oxygen vacancy position in the center. This work, however, reveals a new critical phenomenon: removal of Fe^{3+}–V_O centers at $T=T_c$ results in grain boundaries and increased barriers for carrier motion at $T\geqslant T_c$. The decrease in room temperature resistivity with an increase in Fe^{3+}–V_O center concentration at $x<x_c$ confirms the contribution of these centers to the resistivity jump at $x\leqslant x_c$. Since these centers are effective traps for electrons (transformation of Fe^{3+} to Fe^{2+}) as discussed earlier, they will decrease the conductivity, *i.e.* increase resistivity. Conversely a decrease in their concentration increases the conductivity [see Figs. 3(a) and 4].

On the other hand, an increase in the concentration of Ln^{3+}–Ti^{3+} centers decreases the resistivity [see Figs. 3(b) and 4] indicating Ti^{3+}–Ln^{3+} centers are sources of donor levels, leading to electronic conductivity in samples. Since the formation of Ln^{3+}–Ti^{3+} centers is accompanied by the generation of PTCR properties in doped barium titanate, it can be stated that these centers are present within grains, which have semiconducting properties, rather than at grain boundaries, which are known to have dielectric properties. Unavoidable impurity centers such as Fe^{3+}–V_O produce acceptor electronic levels, which increase the sample resistivity. A decrease in both center concentration and grain size [Figs. 3(a) and 9] also suggests that Fe^{3+}–V_O centers are within the grains. Moreover, because grain boundaries are known to be enriched by oxygen the existence of Metal–V_O centers at such positions would be unlikely. The destruction of these centers at $T=T_c$ would enrich the intergrain space with impurities and hence increase the barriers and sample resistivity. The dipole moments of the Ti^{3+}–Ln^{3+}, Fe^{3+}–V_O and Ln^{3+}(A)-Ln^{3+}(B) centers can induce a nonzero electric field in the lattice and so the presence of an electric field can decrease the varistor effect with increasing rare-earth ion concentration (see Fig. 6).

In summary, the Fe^{3+}–V_O and Ti^{3+}–Ln^{3+} centers revealed in this work in rare-earth ion doped $BaTiO_3$ ceramics play a decisive role in resistivity and PTCR properties of the materials. Since Fe^{3+}–V_O centers exist only at $x<x_c$ and Ti^{3+}–Ln^{3+} centers have a maximum concentration near $x=x_c$ the critical concentration, x_c can be considered as the boundary concentration for the jump of resistivity. The data in Fig. 5 confirm this statement.

References

1 H. Ikushima, *J. Phys. Soc. Jpn.*, 1966, **21**, 1866.
2 T. Miki and A. Fujimoto, *J. Appl. Phys.*, 1998, **83**, 1592.
3 S. Jida and T. Miki, *J. Appl. Phys.*, 1996, **80**, 5234.
4 T. R. N. Kutty and P. Murugaraj, *Mater. Lett.*, 1985, 195.
5 M. D. Glinchuk, I. P. Bykov, V. M. Kurliand, M. Boudys, T. Kala and K. Nejezchleb, *Phys. Status Solidi A*, 1990, **122**, 341.
6 I. P. Bykov, M. D. Glinchuk, V. G. Grachev, Yu. V. Martinov and V. V. Skorokhod, *Fiz. Tverd. Tela*, 1991, **33**, 3459 (in Russian).
7 M. T. Buscaglia, V. Buscaglia, M. Viviani, P. Nanni and A. M. Ferrari, *Doping of $BaTiO_3$ with Rare-earth Oxides/ CIMTEC '98—9th International Conference on Modern Materials and Technologies*, Florence, Italy, 1998.

8 M. T. Buscaglia, M. Viviani and P. Nanni, *Atomistic Simulation Study of Dopant Substitution in $BaTiO_3$/101st ACerS Annual Meeting & Expo.*, Indianapolis, 1999.
9 M. Drofenik, *J. Am. Ceram. Soc.*, 1993, **76**, 123.
10 Y. P. Kostikov and B. B. Leykina, *Izv. AN SSSR. Inorg. Mater.*, 1985, **21**, 1915 (in Russian).
11 T. Sakudo, *J. Phys. Soc. Jpn.*, 1963, **18**, 1626.
12 W. R. Eliot and J. L. Bjorkstam, *J. Phys. Chem. Solids*, 1964, **25**, 1273.
13 A. W. Hornig, R. C. Rempel and H. E. Weaver, *J. Phys. Chem. Solids*, 1959, **10**, 1.
14 E. Possenriede, P. Jacobs and O. F. Shirmer, *J. Phys.: Condens. Matter*, 1992, **4**, 4719.
15 E. Siegal and K. A. Muller, *Phys. Rev. B*, 1977, **19**, 109.
16 R. Vivekanadan and T. R. N. Kutty, *Mater. Sci. Eng. B*, 1990, **6**, 221.
17 P. Murugaraj and T. R. N. Kutty, *J. Mater. Sci. Lett.*, 1986, **5**, 171.
18 B. Scharfschwerdt, A. Mazur, O. F. Shirmer, H. Hesse and S. Mendricks, *Phys. Rev. B*, 1996, **54**, 15284.
19 C. A. Kleint, U. Stopel and A. Rost, *Phys. Status Solidi A*, 1989, **115**, 165.
20 T. Murakami, T. Mijashita, M. Naakahara and E. Sekine, *J. Am. Ceram. Soc.*, 1973, **56**, 294.
21 C. H. Park and D. J. Chadi, *Phys. Rev.*, 1998, **57**, R13961.
22 A. E. Krumin, *Phase Transitions and its Peculiarities in Ferroelectrics*, Riga University, 1984, pp. 3–63 (in Russian).
23 L. A. Xue, Y. Chen and R. J. Brook, *Mater. Sci. Eng.*, 1988, **B1**, 193.
24 T. R. N. Kutty, P. Murugaraj and N. S. Gajbhaye, *Mater. Lett.*, 1984, **2**, 396.
25 D.Macovec, Z. Sumardzija, U. Delaut and D. Kolar, *J. Am. Ceram. Soc.*, 1995, **78**, 2193.
26 G. V. Levis and C. R. A. Catlow, *J. Phys. Chem. Solids*, 1986, **47**, 89.
27 W. H. Shin and Q. Lu, *Ferroelectrics*, 1994, **154**, 241.
28 M. D. Glinchuk and V. A. Stephanovich, *J. Phys.: Condens. Matter*, 1994, **6**, 6317.
29 W. Heywang, *Solid State Electron*, 1961, **3**, 51.
30 C. H. Jonker, *Solid State Electron*, 1964, **7**, 895.

Paper a909647g